On the Performance Anomaly in WiMAX networks

Andrea Detti, Pierpaolo Loreti, Remo Pomposini

University of Rome "Tor Vergata", Electronic Engineering Dept., Italy

{andrea.detti, pierpaolo.loreti, remo.pomposini}@uniroma2.it

***Abstract*— The WiMAX system carries a wide range of services in urban and rural environments supporting quality of service. A key element of the QoS framework is the scheduling algorithm adopted by the Base Station (BS). In this paper we analyze the saturation throughput perceived by Mobile Stations in the cases of two BS scheduling algorithms: Deficit Round Robin (DRR) and time-based DRR.**

We demonstrate that the WiFi issue of "Performance Anomaly" also occurs in WiMAX networks: when the BS uses scheduling approaches aimed at achieving throughput-fairness, like DRR. Performance Anomaly means that when some Mobile Stations (MSs) use a very low bit rate, the throughput of MSs with a high bit rate is dramatically degraded.

We propose time-based DRR as a viable solution to remove the Performance Anomaly. Time-based DRR is a simple modification of the DRR algorithm that achieves time-fairness. Its implementation is feasible in WiMAX.

The analysis is carried out by means of analytical models supported by NS2 simulations. Two scenarios are considered: the first is suitably setup to highlight and to understand the phenomenon of Performance Anomaly; the second examines the impact of Performance Anomaly on a system level focusing on a rural environment.

I. INTRODUCTION

The IEEE 802.16 is a wireless standard for long distance broadband access. The WiMAX forum organization has developed a certification program that ensures the interoperability of products based upon the IEEE 802.16. A device that is awarded the certification is tagged as a "WiMAX" device.

Since 2001, the 802.16 standardization activity has extended the scope of the IEEE 802.16 technology mostly in terms of operative frequency bands and of mobility support. Nowadays two families of products can obtain the WiMAX forum certification: devices based on the standard IEEE 802.16-2004 (Fixed WiMAX) [1] and devices based on the amendment IEEE 802.16e-2005 (Mobile WiMAX) [2]. Among the two families, the Mobile WiMAX seems the future choice, since it is able to efficiently manage both fixed and mobile environments.

The WiMAX systems are based on point-to-multipoint (PMP) architecture with a Base Station (BS) and a set of Mobile Stations (MSs). WiMAX BSs can be deployed either to build a cellular network or to provide hot-spots coverage in particular areas. WiMAX MSs may be fixed Customer Premises Equipment (CPE) or "mobile chips" integrated within laptop computers and mobile devices. The radio coverage of fixed CPEs can reach tens of kilometers using directional antennas (e.g. roof-top antennas) providing line-of-sight propagation. On the contrary, in the case of mobile chips, the BS-MS service distance is strongly reduced to the order of kilometers, since the radio propagation is mostly not in line-of-sight.

WiMAX technology may be deployed both in cities and in rural environments. Within a city, WiMAX may be the technological medium for emerging operators that intend to enter in the broadband market. Nevertheless, in this sector mobile 3G and fixed xDSL carriers may be effective competitors. In rural environments the population density is very low and WiMAX seems a viable technology for bridging the digital divide, since the presence of broadband carriers is limited. Due to the scarce population density, to obtain an investment gain we foresee that the operator will deploy the network adopting the hot-spot paradigm. In addition, a single hot-spot will cover a wide area, so that the profits obtained by the gathered traffic balances the infrastructure investment. Consequently, in rural scenarios the MSs will probably be fixed CPEs.

WiMAX is effective in carrying a wide range of services supporting quality of service. This is done by means of i) a standardized protocol framework and ii) scheduling algorithms that are not specified in the standard. This fact leaves the manufacturers free to customize their products and stimulates the research community in devising suitable scheduling techniques.

QoS management is centrally performed by the BS that controls the downlink and uplink radio resources. Moreover, the BS can take into account the channel quality of each MS and assign a

modulation and coding scheme that maximizes the *transmission bit rate*; that is the useful bit rate available at MAC layer.

In this paper we demonstrate that if the BS uses a scheduling approach that is fair in terms of the bits exchanged per MS in the unit time, the "Performance Anomaly" phenomenon appears. Performance Anomaly is the fact that an MS that uses a low transmission bit rate (e.g. the modulation method QPSK 1/2) captures the radio medium for a long time and, consequently, penalizes other MSs that use higher bit rate (e.g. 64 QAM 3/4) and the overall network throughput, as well.

The Performance Anomaly is already modeled for WiFi networks [3] but, differently from WiFi, the Performance Anomaly is not a "pathological" issue of the WiMAX system, since it derives from the choice of a specific scheduling approach. For this reason, the Performance Anomaly can be faced by properly designing the scheduler, without modifying the IEEE 802.16 standard. Moreover, the WiMAX Performance Anomaly is relevant only for the Best Effort traffic, which does not require any level of QoS. For other QoS classes, the fact that an MS may capture the radio medium for a long time is not an issue, but is a consequence of the QoS agreement.

In order to model the Performance Anomaly, we analytically evaluate the saturation throughput of Best Effort downlink connections, when the BS uses a Deficit Round Robin (DRR) scheduler. Afterwards, to evenly reduce that performance degradation, we propose a simple modification of the DRR that leads the system to be fair in terms of time, instead of throughput. We name this algorithm "time-based DRR" and we model the saturation throughput of Best Effort downlink connections also in this case. We assess the developed models by means of NS2 simulations.

Although we have considered only downlink traffic, the qualitative results obtained in this case can also be extended: i) to the case of uplink Best Effort traffic, since the MAC layer physically separates uplink and downlink direction, thus the same phenomena occur in uplink; ii) to the case in which there are also other kinds of service flows (e.g. UGS); in fact, in this case the Best Effort classes will use only a part of the available radio capacity, hence the absolute results will be scaled but the performance trend does not change.

The paper is organized as follows: section II summarizes the WiMAX scheduling issue in order to focus the present work within the WiMAX system. Section III depicts the WiMAX reference scenario we considered, and it describes the adopted DRR algorithms. Section IV reports on the analytical models of the saturation throughput for both DRR and time-based DRR schedulers. Section V reports on the performance evaluation assessing the analytical models and quantifying the Performance Anomaly in different scenarios. Finally conclusions are drawn.

II. BACKGROUND ON WIMAX SCHEDULER

The resource allocation performed by the BS scheduler should satisfy the QoS requirements of the active *service flows*. A service flow is a connection-oriented MAC service that offers unidirectional transport of data packets. A service flow is characterized by a set of QoS parameters such as latency, jitter, and throughput assurances.

The Mobile WiMAX standard [2] introduces five type of *data delivery services* that can be considered as QoS classes: Unsolicited Grant Service (UGS), Real-time variable-rate service (RT-VR), Non-real-time variable-rate service (NRT-VR), Extended real-time variable-rate service (ERT-VR) and Best Effort (BE).

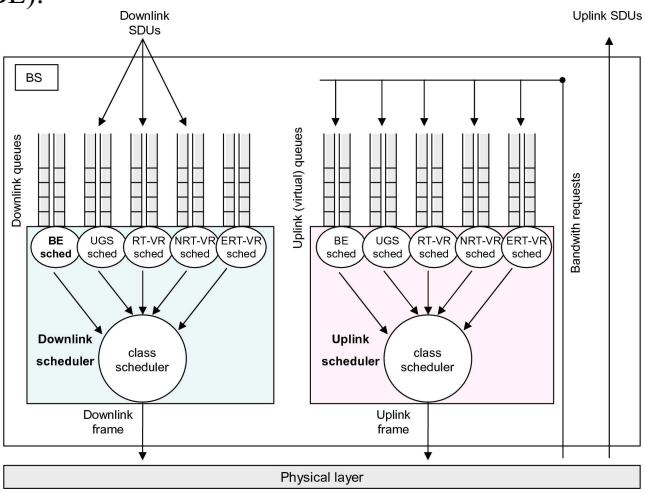

Fig. 1 – A possible WiMAX BS scheduler blueprint.

The UGS class is designed to support real time applications that generate fixed-size packets at periodic intervals with stringent delay requirements. The RT-VR and ERT-VR classes are designed to support real time applications that generate variable-size packets at periodic intervals with moderate delay requirements; ERT-VR is better at supporting traffic with silence suppression. The NRT-VR class is designed to support delay tolerant traffic, such as file transfer, with a minimum guaranteed bandwidth.

Finally, the Best Effort (BE) class is designed to support delay tolerant traffic without any guaranteed delay and bandwidth.

In Fig. 1 we report a possible blueprint of the functional entities for QoS support, which logically reside within the MAC layer of the BS [4].

In the downlink direction, there is a dedicated queue for each service-flow. The queues are drained on a frame basis by the "downlink scheduler". In the uplink direction, the matter is more complex. The MSs indicate resources needed per service flow by a bandwidth request mechanism (with the exception of the UGS service flows that have a fixed assigned capacity). The "uplink scheduler" should reserve the bandwidth for the uplink service flows that are backlogged. The scheduler first allocates the capacity for the UGS traffic and then for the other service flows according to the QoS agreement. Although bandwidth requests are on a service flow basis, the BS usually grants uplink bandwidth per MS. Thus, also the MS has to implement an internal scheduler that shares the allocated capacity among the active service flows.

The main research challenge on the scheduler is the design of downlink and uplink scheduling algorithms that guarantee the QoS. Since the Mobile WiMAX standard defines five QoS service classes (i.e., *data delivery services*), most of these algorithms are oriented to a hierarchical queuing approach [4][5][6][7]. The scheduler first shares the whole bandwidth among QoS classes and then, within a QoS class, shares the resources among the service flows.

III. Reference scenario and Analyzed Scheduling techniques

This section describes the reference scenario and the scheduling techniques considered in this paper.

We consider a Mobile WiMAX interface characterized by the physical parameters reported in Tab. 1. The network topology consists of a set of MSs served by a BS. MSs may use different modulation methods, i.e. different transmission bit rates. Each MS has a single Best Effort data connection (i.e. a service flow) in the downlink direction. This connection is used to transfer data from a source located on the BS. The data source is *greedy*, i.e. the downlink queue dedicated to the MS data connection is never empty.

Tab. 1 – System parameters

Parameters	*Values*
System bandwith	5 MHz
Permutation scheme	PUSC
Sampling frequency	5.6 MHz
FFT size	512
N. of Downlink Sub-Channels	15
N. of Uplink Sub-Channels	17
OFDMA symbol duration	102.86 μs
Frame duration	5 ms
GT=RTG+TTG (guard times)	0.3571 ms
DL_Ratio	0.48

On the BS, we consider two scheduling techniques for downlink Best Effort traffic (Fig. 1): DRR [8] and time-based DRR. We chose the DRR approach since it fulfils the necessity of draining packets from a set of queues and it is a simple and feasible technique which might be implemented in the WiMAX BS [9].

We briefly describe the DRR algorithm: the scheduler loops among all non-empty queues. During a loop and when the *i*-th queue is selected, the following actions occur: i) the scheduler increases the *deficit counter* of the *i*-th queue with a constant amount of bits, named *quantum*; ii) it serves the head-of-line packet, if the size of this packet is lower than the deficit counter; after that the deficit counter is decreased by the packet's size and the next head-of-line packet is handled; iii) when no more packets can be served from the *i*-th queue, the queue *i+1*-th is selected. On average, each queue obtains the same amount of bits per unit time (i.e. the same throughput).

Time-based DRR is a configuration of the DRR[1] that shares fairly the time utilization of the radio interface instead of the throughput [14]. We implement this modification by weighting the quantum of the *i*-th queue (i.e. *Q(i)*) as follows:

$$Q(i) = const \cdot \frac{bpst(i)}{\max(bpst)} \quad (1)$$

where *bpst*(*i*) is the number of bits per OFDMA slot achieved with the modulation method of the *i*-th MS. Instead max(*bpst*) is the number of bits per OFDMA slot achieved with the most efficient modulation method (i.e. 64 QAM 3/4). Since BS knows the modulation method of each data connection the time-based DRR is feasible.

Finally, we discuss a scheduling approach for

[1] It may also be seen as a Weighted Deficit Round Robin (WDRR)

uplink traffic that may be adopted to implement the DRR and time-based DRR algorithms. In uplink, the BS does not know the size of packets that are backlogged, but only the overall amount of backlogged bytes per data connection. This prevents a strict implementation of the DRR approach, which indeed works on a packet-base. Therefore, the uplink scheduler in the BS can only approximate a DRR algorithm. We propose a DRR implementation based on the following approximation: all uplink packets have a fixed size L, equal to the expected mean. Thus, considering a queue that has B backlogged bytes, the scheduler works as if there were $\lfloor B/L \rfloor$ packets of length L and a packet of length $B-\lfloor B/L \rfloor L$ (the brackets $\lfloor\ \rfloor$ indicate the floor operator).

IV. ANALYTICAL MODELS

In this section we analytically derive the saturation throughput[2] of downlink data connections with DRR and time-based DRR schedulers.

Firstly we evaluate the saturation throughput as a function of the quantum $Q(i)$; then we use the specific values of $Q(i)$ to evaluate the saturation throughput for the DRR and the time-based DRR.

In order to simplify the analysis we use a fluidic approach by assuming that the amount of packets stored in a queue is an amount of fluid, measured in bits. Moreover, we assume that the scheduler is able to drain any part of this fluid, independently of the packets' boundaries. In Section V, we asses the validity of these assumptions through NS2 simulations.

We define a *DRR round* as a complete cycle of the scheduler among all downlink queues. Moreover, we define *NRF* as the average number of DRR rounds that occur in a WiMAX frame. The WiMAX frame has a duration of T_f seconds.

Since sources are greedy, downlink queues are never empty, therefore, during a DRR round the scheduler drains $Q(i)$ bits from each queue. Consequently, the average number of useful bits transferred versus the i-th MS in the unit time (i.e. the throughput $Th(i)$) can be written as:

$$Th(i) = \rho\ Q(i) \frac{NRF}{T_f} \tag{2}$$

where ρ is an efficiency factor (less or equal to one) that accounts for protocols overheads. Therefore, the factor ρ is defined as the ratio between the number of useful bits transferred in a packet and the overall length of the packet.

The average number of DRR rounds per frame (*NRF*) can be written as:

$$NRF = \frac{N_{uds}}{N_{spr}} \tag{3}$$

where N_{uds} is the average number of useful downlink OFDMA slots in a frame, and N_{spr} is the number of downlink OFDMA slots required to transmit all the bits of a DRR round. In following we evaluate first N_{spr} and then N_{uds}.

Considering that in each DRR round the scheduler drains $Q(i)$ bits from each queue, it follows that the number of downlink OFDMA slots per round (N_{spr}) is equal to

$$N_{spr} = \sum_{i=1}^{M} \frac{Q(i)}{bpst(i)} \tag{4}$$

where M is the number of queues (i.e. of MSs) [3].

The evaluation of $bpst(i)$ can be obtained considering that a downlink OFDMA slot in case of PUSC permutation is defined as one downlink sub-channel over two OFDMA symbols. One downlink sub-channel is formed by 24 useful sub-carried. Therefore,

$$bpst(i) = 48\, bms(i)\, cr(i) \tag{5}$$

where *bms(i)* is the number of bits per modulation symbol and *cr(i)* is the coding rate. For instance, in case of QPSK 1/2 we have: *bms* = 2 and *cr* = 0.5. In Tab. 2 the values of *bpst* for each type of modulation methods are reported.

TAB. 2 – NUMBER OF BITS PER OFDMA SLOT (BPST) WITH A PUSC PERMUTATION SCHEME

Modulation method	*bpst*
QPSK 1/2	48
QPSK 3/4	72
16 QAM 1/2	96
16 QAM 3/4	144
64 QAM 1/2	144

[2] The saturation throughput is defined as the useful data rate obtained in presence of greedy sources.

[3] We are neglecting the fact that the bandwidth allocation performed on the radio interface is an integer number of OFDMA slots.

64 QAM 2/3	192
64 QAM 3/4	216

The average number of useful downlink OFDMA slots in a downlink sub-frame (N_{uds}) can be written as:

$$N_{uds} = \left\lfloor N_{subch\_DL} \frac{(N_{sym\_DL} - N_{sym\_DL\_oh})}{2} \right\rfloor \quad (6)$$

where N_{subch_DL} is the number of downlink sub-channels, N_{sym_DL} is the total number of downlink symbols per frame, $N_{sym\_DL\_oh}$ is the average number of downlink overhead symbols used to transmit signaling messages (preambles, FCH, DLMAP, ULMAP, DCD and UCD) and the factor 2 account that a downlink PUSC slot last two symbols.

The value of N_{subch_DL} is a system parameter and the value of N_{sym_DL} can be calculated as:

$$N_{sym\_DL} = \lfloor N_{sym} \cdot DL\_Ratio \rfloor \quad (7)$$

where the *DL_Ratio* is reported in Tab. 1. N_{sym} is the number of OFDMA symbols in a frame evaluated as:

$$N_{sym} = \left\lfloor \frac{T_f - GT}{T_s} \right\rfloor \quad (8)$$

where T_f is the frame duration, GT is the guard time and T_s is the OFDMA symbol duration.

The calculation of $N_{sym\_DL\_oh}$ in Eq. (6) is not an easy task, since it depends on the traffic pattern and on the scheduling approach. For this reason, we follow the approximation adopted in [10] assuming that $N_{sym\_DL\_oh}$ is equal to 4 OFDMA symbols.

We conclude the derivation of N_{uds} observing that in our reference scenario (see Tab. 1) the value of N_{uds} is equal to 127.

Up to now we have derived the saturation throughput for a generic quantum $Q(i)$. Now we specify the evaluation for the values of $Q(i)$ adopted by DRR and by time-based DRR.

In case of DRR, we have that $Q(i) = const$ and the saturation throughput (Th_{DRR}) in Eq. (2) can be written as:

$$Th_{DRR}(i) = Th_{DRR} = \left(\rho \frac{N_{uds}}{T_f} \right) \left(\sum_{j=1}^{M} \frac{1}{bpst(j)} \right)^{-1} \quad (9)$$

As expected, $Th_{DRR}(i)$ is independent of i, indicating that all MSs obtain the same throughput. Moreover, the saturation throughput depends on the number of MSs (M) but it also depends on the modulation method of all MSs ($bpst(j)$). This dependence implies that the saturation throughput of the i-th MS decreases when another j-th MS reduces its transmission bit rate (i.e. lower values for $bpst(j)$).

In case of time-based DRR we have that $Q(i)$ follows Eq. (1) and the saturation throughput ($Th_{TB\text{-}DRR}$) in Eq. (2) can be written as:

$$Th_{TB-DRR}(i) = \left(\frac{\rho \, N_{uds} \max(bpst)}{T_f \; const} \right) \frac{bpst(i)}{M} \quad (10)$$

The saturation throughput $Th_{TB\text{-}DRR}(i)$ depends on the transmission bit-rate (i.e. on $bpst$(i)) of the i-th MS and on the number of MSs (M). Differently from $Th_{DRR}(i)$ in Eq. (9), $Th_{TB\text{-}DRR}(i)$ does not depend on the transmission bit rate of the other MSs.

Finally, we observe that in presence of QoS traffic the parameter N_{uds} in Eqs. (9) and (10) has to be reduced to the effective number of ODFMA slots available for BE traffic.

V. PERFORMANCE EVALUATION

In this section we evaluate the system performance in two topological scenarios. The first one is formed by a set of MSs transmitting at a high bit rate (i.e. $bpst$ = 216) and by one MS whose bit rate is varied. Such a setup allows us to highlight and to explain the phenomenon of Performance Anomaly. The second scenario is formed by a set of MSs randomly distributed in a rural environment and the average distance BS-MS is varied. A scenario like this is useful to evaluate the impact of Performance Anomaly at a system level.

The performance evaluation is carried out using both the model developed in the previous section and using NS2. In particular, we selected NS2 version 2.31 with the following add-on: i) 802.16d WiMAX module, developed by NIST [11]; ii) some specific modifications of the NIST module developed by us in order to simulate the 802.16e OFDMA interface, the DRR and the time-based DRR schedulers.

A simulation runs for 250s and the traffic is generated in the last 120s. Each simulation is repeated 20 times varying the random seed. The 95% confidence interval is evaluated.

In the following we report the results obtained for both scenarios. The following plots show that there is a high degree of similarity between the analytical expressions (Eq. (9) and Eq. (10)) and the simulation results; hence we avoid commenting this fact further.

A. Scenario 1

We consider M mobile stations. The MS n.1 alternatively uses three different modulation methods: QPSK 1/2, 16 QAM 3/4 and 64 QAM 3/4. The other M-1 MSs use the 64 QAM 3/4 modulation method.

We first analyze the performance with DRR and then with time-based DRR.

In all plots of this scenario the confidence intervals are not reported since the system randomness are very limited and the confidence interval results smaller than plot markers.

1) DRR scheduler

In Fig. 2 we report the saturation throughput[5] of a generic MS versus the number of mobile nodes M. We recall that, due to the presence of the DRR, all MSs have the same performance in terms of throughput.

Let us now discuss these performances assuming that they are related to MS n.2, i.e. an MS with a high transmission bit rate. When there are only two MSs, the performance of MS n.2 is strongly related to the modulation method of MS n.1. For instance, when MS n.1 uses a 64 QAM 3/4 (as used by MS n.2.), MS n.2 has a saturation throughput of about 2.7 Mbps. Instead, when MS n.1 uses a QPSK 1/2, the saturation throughput of MS n.2 is strongly reduced to about 1 Mbps. This is evidence of the Performance Anomaly, since the performance of a high speed MS is strongly degraded by the presence of a low bit rate MS. Obviously, increasing M, the number of high speed MSs increases and the impact of the modulation method of MS n.1 decreases as well.

[5] That is the throughput obtainable with greedy sources

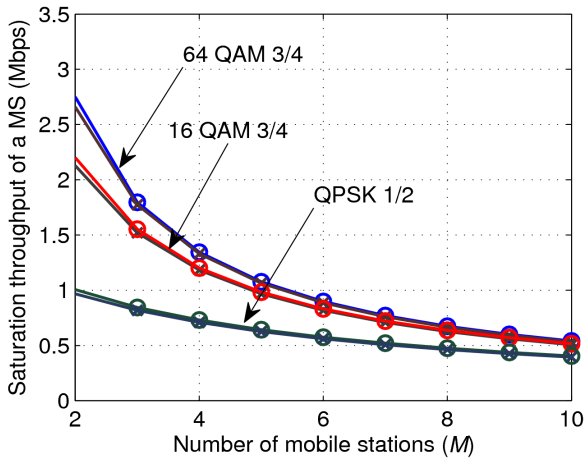

Fig. 2 – Saturation throughput of a generic MS versus the number of MSs (M) with DRR; MS n.1 uses three different modulation methods (64 QAM 3/4 , 16 QAM 3/4, QPSK 1/2), other MSs always use 64 QAM 3/4; simulation (O) and analytical (X) results.

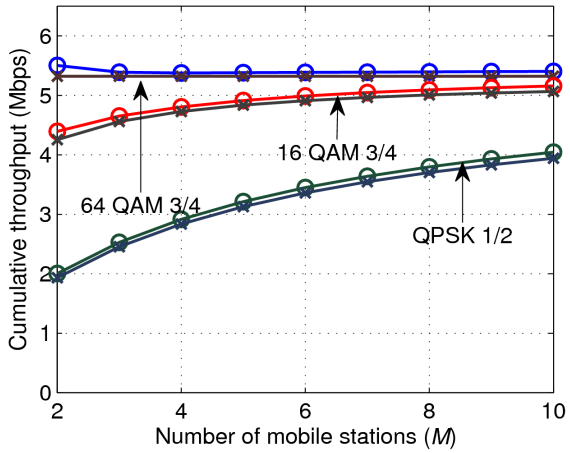

Fig. 3 – Cumulative saturation throughput with DRR; MS n.1 uses three different modulation methods (64 QAM 3/4 , 16 QAM 3/4, QPSK 1/2), other MSs always use 64 QAM 3/4; simulation (O) and analytical (X) results.

In Fig. 3 we report the cumulative saturation throughput; i.e. the sum of the saturation throughput for all MSs. As expected, the reduction of the transmission bit rate of MS n.1 reduces the cumulative throughput as well, but this effect tends to vanish increasing the number of high speed MSs.

2) Time-based DRR scheduler

In Fig. 4 and Fig. 5 we report the saturation throughput of MS n.2 and of MS n.1 versus the number of mobile stations M.

Fig. 4 shows that the saturation throughput of MS n.2 is independent of the transmission bit rate of MS n.1, but only depends on the number of mobile

stations (M) and decreases as $1/M$. This is due to the time-based DRR, which, in presence of M mobile stations serves MS n.2 for $1/M$ of the frame duration, independently of the transmission bit rate of other MSs. Since the transmission bit rate of MS n.2 is unvaried, the curves for different modulation methods of MS n.1 overlap themselves.

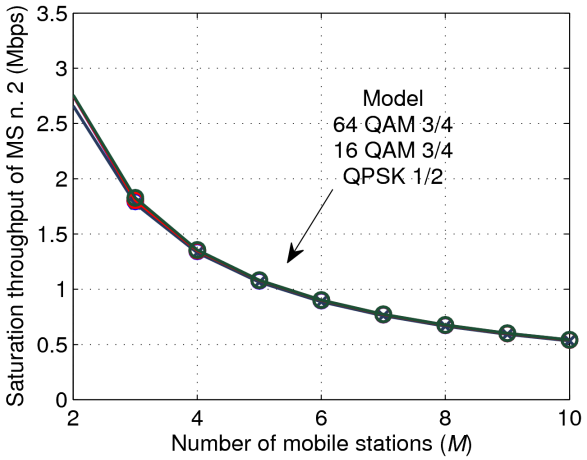

Fig. 4 – Saturation throughput of MS n.2 versus the number of MSs (M) with time-based DRR; MS n.1 uses three different modulation methods (64 QAM 3/4 , 16 QAM 3/4, QPSK 1/2), other MSs always use 64 QAM 3/4; simulation (O) and analytical (X) results.

In Fig. 5 we report the saturation throughput of MS n.1 versus the number of mobile nodes M. As for MS n.2, for a given modulation method the saturation throughput decreases as $1/M$. Moreover, the decrease of the transmission bit rate of MS n.1 (i.e. the decrease of the number of bits per modulation symbol) leads to a decrease of the saturation throughput of that MS. In fact, fewer bits can be transferred in the frame time interval reserved for that MS.

It worth comparing the performance experienced by MS n. 2 for the two different DRR schedulers. Let us assume that M equals to 2 and the modulation method QPSK 1/2 for MS n.1. With DRR MS n.2 has a saturation throughput of about 1 Mbps (see Fig. 2), that is equal to the saturation throughout of MS n.1. With time-based DRR, MS n.2 has a saturation throughput about three times greater and it is about 2.7 Mbps; at the same time, the benefits obtained by MS n.2 are offset a little by MS n.1, whose saturation throughput is about 600 kbps.

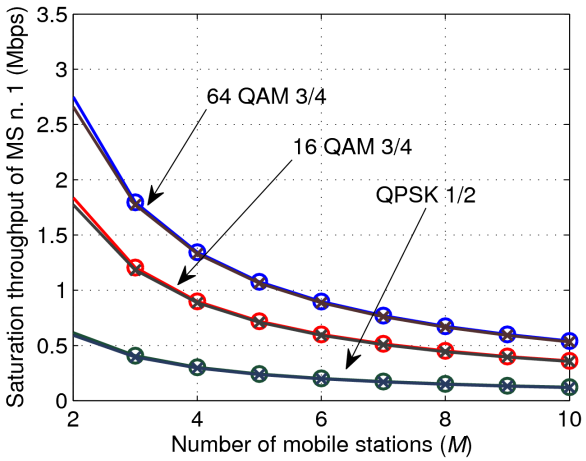

Fig. 5 – Saturation throughput of MS n. 1 versus the number of MSs (M) with time-based DRR; MS n.1 uses three different modulation methods (64 QAM 3/4 , 16 QAM 3/4, QPSK 1/2), other MSs always use 64 QAM 3/4; simulation (O) and analytical (X) results.

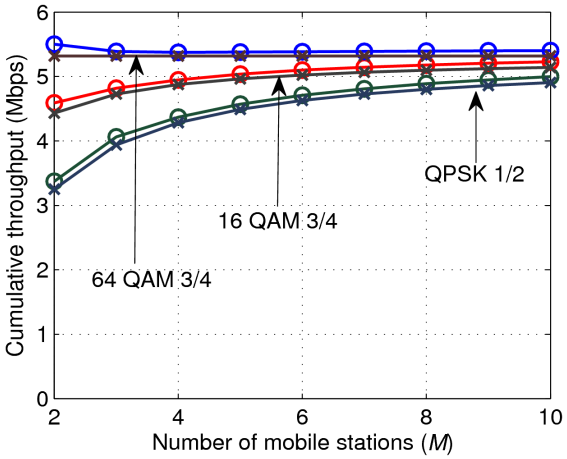

Fig. 6 – Cumulative saturation throughput with time-based DRR; MS n.1 uses three different modulation methods (64 QAM 3/4 , 16 QAM 3/4, QPSK 1/2), other MSs always use 64 QAM 3/4; simulation (O) and analytical (X) results.

Finally, Fig. 6 reports the cumulative saturation throughput for a time-based DRR scheduler. The presence of an MS with low transmission rate (i.e. MS n.1) reduces the cumulative throughput. Anyway, with respect to the DRR case (see Fig. 3), this reduction is more limited and the throughput is higher. This is due to the fact that, with time-based DRR, the decrease of the transmission bit rate of MS n.1 only lowers its own throughput, not affecting the saturation throughputs of the other MSs.

B. Scenario 2

We consider 10 MSs randomly located in a sector covered by a BS antenna. The distance between an

MS and the BS is a random variable with a negative exponential distribution. In order to guarantee that all MSs are within the radio coverage of the BS, the negative exponential is limited to a maximum value R_{max} that is equal to the maximum transmission range achievable with the smaller transmission rate (i.e. modulation method QPSK 1/2). The limitation is performed in this way: if the extracted distance value is greater than R_{max}, the returned value is R_{max}. In doing so, the average distance R_{mean} MS-BS is equal to:

$$R_{mean} = \lambda - \lambda e^{-\frac{R_{max}}{\lambda}}. \quad (11)$$

where λ is the parameter of the unlimited exponential distribution.

Through a link budget we derive a relation between the modulation method and BS-MS distance; this relation is used within the NS2 simulation scripts to set the modulation method of MSs. Clearly, different modulation methods require different target signal to noise ratios at the receiver. The link budget parameters are reported in [10]. For simplicity, we assume that only three modulation methods are available: QPSK 1/2, 16 QAM 3/4 and 64 QAM 3/4.

TAB. 3 – PHYSICAL PARAMETERS ADOPTED FOR LINK BUDGET

Parameter	*Value*
FREQUENCY BAND	3.5 GHz
TX POWER (PTX)	43 dBm
TX ANTENNA GAIN (GTX)	15 dB
RX ANTENNA GAIN (GRX)	3 dB
MARGIN (MN)	10 dB
KT_0	-174 dBm
NOISE FIGURE (F)	10 dB
NOISE BANDWIDTH (B)	67.50 dB
TARGET SNR QPSK 1/2	5 dB
TARGET SNR 16 QAM 3/4	14 dB
TARGET SNR 64 QAM 3/4	20 dB

In Tab. 4 we report the parameters used to calculate the propagation loss using the Erceg channel model. The Erceg models rural WiMAX path loss in case of fixed CPEs [12][13].

In Tab. 5 we report the MS-BS distance ranges for the different modulation methods derived from link budget parameters of and with the Erceg path-loss model. For example, if the MS exponentially generated distance fall in the first range a 64 QAM 3/4 modulation method is used for the communication.

TAB. 4 – ERCEG MODEL PARAMETERS

Parameter	*Value*
Base station altitude	70 m
Shadowing factor	10.2 dB
Terrain Type	C

TAB. 5 – DISTANCE RANGE PER MODULATION METHOD

Distance Ranges (km)	*Modulation*
0 – 29	64 QAM 3/4
29 – 36	16 QAM 3/4
36 – 48 (R_{max})	QPSK 1/2

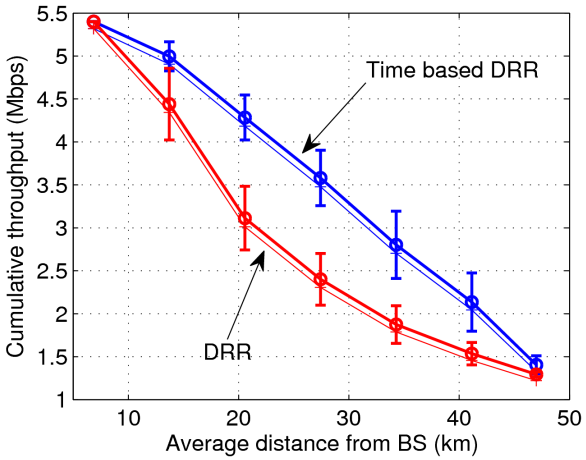

Fig. 7 – Cumulative saturation throughput for the DRR and the time based DRR as a function of the average MS-BS distance; simulation (O) and analytical (+) results.

Fig. 7 reports the cumulative saturation throughput with DRR and time-based DRR schedulers varying the average BS-MSs distance R_{mean}. As expected when the MSs are all near to (i.e. R_{mean} = 6 km), or all distant (i.e. R_{mean} = 47 km) from, the BS, MSs use the same modulation method and both schedulers perform equally. On the contrary, for intermediate distance values, slow and fast MSs are present and the Performance Anomaly degrades the cumulative saturation throughput with the DRR scheduler. This degradation is significantly further limited when using time-based DRR.

Up to now we have measured the performance anomaly phenomenon thought a saturation analysis. In the next, we extend the analysis varying the traffic load. Such an analysis is carried out only by means of simulations. We chose an average distance R_{mean}

equals to 27.5 km. For each MS, we set up a downlink Poisson source that generates packets of fixed length (1460 bytes) with packet interarrival time regulated by a negative exponential distribution. The average packet interarrival time depends on the considered traffic load. For each MS, the BS allocates a BE downlink queue of 100 packets (Fig. 1).

Fig. 8 reports the delivery ratio and the latency versus the overall traffic load measured in Mbps. The delivery ratio is the fraction of received packets versus to the sent ones and the latency is the time elapsed between the packet generation and its reception.

We observe that the time-based DRR improves the system performance and such improvement is as greater as more traffic is offered. This is a direct consequence of the better usage of the radio resource performed by time-based DRR.

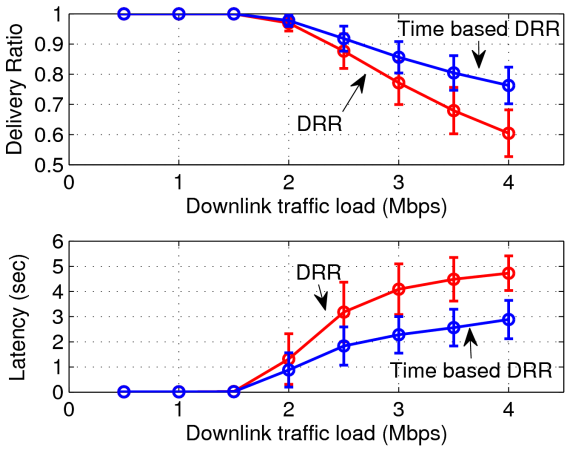

Fig. 8 – Delivery ratio and latency in case of downlink Poisson sources for the DRR and the time based DRR versus the downlink traffic load.

VI. Conclusion

In this paper we have demonstrated that the WiFi Performance Anomaly phenomenon can also occur in WiMAX systems when the Best Effort scheduler is devised for *throughput fairness* among MSs (e.g. DRR). In fact, such a scheduler gives a greater part of the WiMAX frame to MSs with low transmission rate, with respect to the portion given to MSs with high transmission bit rate. As a consequence, the throughput of high speed MSs is strongly reduced.

This issue can be solved by using a scheduler devised for *time fairness* among MSs (e.g. time-based DRR). Removing the time unfairness, MSs with a high transmission bit rate are served for more time and this leads to: i) a significant increase of their saturation throughput (e.g. from 1 Mbps with DRR to 2.7 Mbps with time-based DRR) and, ii) a small decrease of the saturation throughput of MSs with low transmission rates (e.g. from 1 Mbps with DRR to 0.7 Mbps with time-based DRR).

From a system point of view, the benefit of time fairness is relevant in scenarios where customers are widely spread on the coverage area (e.g. rural environment) and the most of bandwidth is used for Best Effort traffic.

References

[1] "*IEEE Standard for Local and Metropolitan Area Networks Part 16: Air Interface for Fixed Broadband Wireless Access Systems*," IEEE Std 802.16-2004 (Revision of IEEE Std 802.16-2001), vol., no., pp. 0_1-857, 2004

[2] "*IEEE Standard for Local and metropolitan area networks Part 16: Air Interface for Fixed and Mobile Broadband Wireless Access Systems Amendment 2: Physical and Medium Access Control Layers for Combined Fixed and Mobile Operation in Licensed Bands and Corrigendum 1*," IEEE Std 802.16e-2005 and IEEE Std 802.16-2004/Cor 1-2005 (Amendment and Corrigendum to IEEE Std 802.16-2004) , vol., no., pp. 0_1-822, 2006

[3] M. Heusse, F. Rousseau, G. Berger-Sabbatel, A. Duda, "*Performance anomaly of 802.11b*," Twenty-Second Annual Joint Conference of the IEEE Computer and Communications Societies, INFOCOM 2003, vol.2, pp. 836-843

[4] C. Cicconetti, L. Lenzini, E. Mingozzi, C. Eklund, "*Quality of service support in IEEE 802.16 networks*," IEEE Network, vol.20, no.2, pp.50-55, March-April 2006

[5] M. Hawa, D. W. Petr. "Quality of Service Scheduling in Cable and Broadband Wireless Access Systems," 10th IEEE International workshop on Quality of Service, May 2002, pp. 247-255.

[6] K. Wongthavarawat, A. Ganz, "*Packet scheduling for QoS support in IEEE 802.16 broadband wireless access systems*," Wiley, International Journal of Communication Systems, Vol. 16, No. 1. (18 February 2003), pp. 81-96.

[7] C. Jianfeng, J. Wenhua; W. Hongxi, "*A service flow management strategy for IEEE 802.16 broadband wireless access systems in TDD mode*," IEEE International Conference on Communications, ICC 2005, vol.5, pp. 3422-3426

[8] M. Shreedhar, G. Varghese, "*Efficient fair queueing using deficit round robin*," ACM Conference SIGCOMM '95

[9] C. Cicconetti, A. Erta, L. Lenzini, E. Mingozzi, "*Performance Evaluation of the IEEE 802.16 MAC for QoS Support*," IEEE Transactions on Mobile Computing, vol.6, no.1, pp.26-38, Jan. 2007

[10] "*WiMAX System Evaluation Methodology*" WiMAX Forum, version 1.7, September 2007

[11] Seamless and secure mobility, http://w3.antd.nist.gov/seamlessandsecure.shtml.

[12] V. Erceg, K.V.S. Hari, M.S. Smith, D.S. Baum et al, "*Channel Models for Fixed Wireless Applications*", IEEE 802.16.3 Task Group Contributions 2001, Feb. 01

[13] V. Erceg et. al, "*An empirically based path loss model for wireless channels in suburban environments*," IEEE JSAC, vol. 17, no. 7, July 1999, pp. 1205-1211

[14] X. Liu, E. K. Chong, and N.B. Shroff, "Opportunistic transmission scheduling with resource sharing constraints in wireless networks," IEEE Journal on Selected Area in Communications, vol. 19, no. 10, pp. 2053-2064, Oct. 2001.